AUT Journal of Electrical Engineering

AUT J. Elec. Eng., 53(2) (2021) 213-222
DOI: 10.22060/eej.2021.19463.5396

Design of a Novel Electrochemical Nanobiosensor for the Detection of Prostate Cancer by Measurement of PSA Using Graphene-based Materials

F. Saeidi Tabar[1], M. Pourmadadi1, F.Yazdian[2*], . Rashedi[1]

[1] Department of Biotechnology, School of Chemical Engineering College of Engineering University of Tehran, Tehran, Iran
[2] Department of Life Science Engineering Faculty of New Science and Technologies University of Tehran, Tehran

ABSTRACT: In this work, an aptamer-based electrochemical nanobiosensor has been developed for early detection of prostate cancer. Prostate-specific antigen (PSA) is the most common marker of prostate cancer, and this study aimes to detect this biomarker through electrochemical nanobiosensor-based aptamer, using nanostructures Graphene Oxide/graphitic Carbon Nitride/Gold nanoparticles (GO/g-C_3N_4/Au NPs). The aptamer chains are stabilized on the surface of a glassy carbon electrode (GCE) by Reduced Graphene Oxide, graphitic Carbon Nitride, and Gold nanoparticles (rGO/g-C_3N_4/Au NPs). To ensure the correct operation of the aptamer, a selectivity analysis was taken between five substances, and an electrochemical biosensor designed with good stability and high selectivity, diagnosis the desired analyte (PSA) compared to other materials. For characterization of aptasensor Electrochemical, CV, SQW and, EIS tests were performed to investigate the features of the synthesized nanoparticles, XRD, FTIR, SEM, TEM tests were carried out, and the results indicated that the used nanoparticles were well synthesized. The limit of detection (LOD) is 1.67 pg.ml^{-1} in hexafrrocyanide ($[Fe(CN)_6]^{-3/-4}$) media, this limit of detection is much lower and demonstrates the high ability of the nanobiosensor in early detection of PSA. The designed biosensor needs a short time (about 30 min) to detect the PSA as a symptom of prostate cancer.

Review History:
Received: Jan. 07, 2021
Revised: Apr. 30, 2021
Accepted: May. 10, 2021
Available Online: Sep. 01, 202

Keywords:
Biomarker
Electrochemical Biosensor
Prostate Cancer
Prostate Specific Antigen
Graphene based materials.

1- INTRODUCTION

Prostate cancer is one of the most common cancers in men [1]. Due to the increase of diseases and different types of cancer in today's societies, many requests have been made to increase the early and accurate diagnosis of cancers and diseases. On the other hand, the development of nanotechnology to diagnose the causes of cancer and the use of new methods has led to the study of many researchers in the field of treatment and early detection of cancer [2]. According to research, cancer is one of the leading causes of death in the world today, and can be considered a serious threat to humanity. Prostate cancer, the silent cancer in men, is one of the most common cancers, and its rapid and easy diagnosis are very important as a primary treatment. The available methods for the diagnosis and treatment of cancer, such as chemotherapy, imaging, surgery, etc., are very expensive and can be performed with very advanced facilities and a lot of time [3]. Researchers are always looking for a way to diagnose cancer in a low-cost, accurate, and highly sensitive way, and ultimately increase the life expectancy of the cancer patients [4]. As mentioned, the early detection of prostate cancer is very effective in the early treatment of cancer. Prostate-specific antigen (PSA) is the most important biomarker for the diagnosis of prostate cancer [1]. This antigen is produced in both healthy men and men with prostate cancer, but increases in sick people [1]. If the serum PSA is higher than 4 ng.ml^{-1}, the person is suspected of having prostate cancer and we need to detect this antigen to prevent cancer from continuing [5]. PSA is a glycoprotein produced by cells in the duct of the prostate gland [6]. The presence of more PSA in the blood of men can indicate prostate cancer [7]. Today, biosensors are used as a diagnostic tool for cancer. Biosensors have been considered by researchers due to their high sensitivity to the desired analyte and being cheaper. Biosensors generally include a stabilized biological system that changes the properties of the environment in the presence of the measuring analyte [8]. Each biosensor is composed of three parts: 1) a bioreceptor that reacts with the target substance, which is the analyte, 2) a transducer that converts the receptor's biological response into an identifiable response, and 3) a readout system that displays the final response [8]. Biosensors are classified in terms of receptor and transducer. The receptor part can be antibodies, enzymes, aptamers, and cells, and in terms of transducers, they may include optical, electrochemical, and mass-based techniques [9]. Electrochemical biosensors have been described as a powerful diagnostic tests over the past years. Due to the unique advantages of electrochemical biosensor, such as especially simplicity, high sensitivity and accuracy, significant attempts have been accomplished to develop electrochemical techniques for detection. The basis of electrochemical

*Corresponding author's email:yazdian@ut.ac.ir

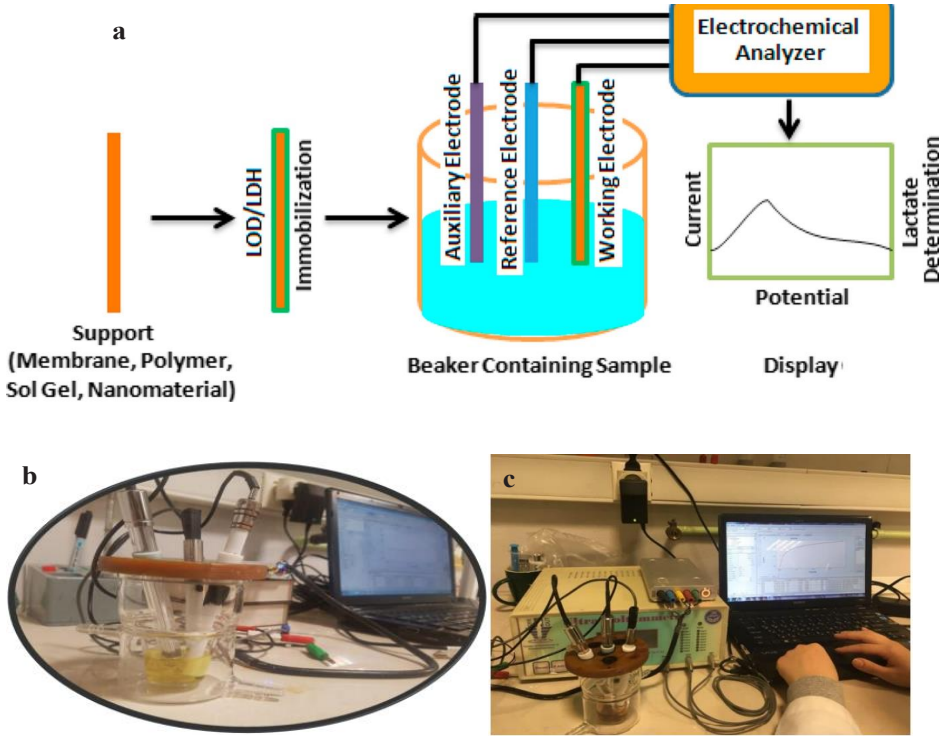

Fig. 1. (a) This illustration depicts the simplicity of a three-electrode electrochemical cell system, Reproduced from Ref [24]. with permission. (b) and (c) show the arrangement of electrodes in real measurements.

biosensors is that an electrochemical reaction takes place between the biomolecule of the receptor and the target molecule, as a result of which an electron is produced or consumed. In these biosensors, the biological element is used as a detection part, and the electron is used as a converter [10]. The reaction in the electrochemical transducer requires a reference, working and counter electrode, and an electrolyte solution [11]. The reference electrode is usually made of Ag/AgCl and is placed near the reaction site to keep the potential at a constant value. The working electrode actually acts as a transducer element and the reaction takes place on its surface. The counter electrode is the interface between the electrolyte solution and the working electrode, so that current reaches the working electrode. These two electrodes must be conductive, thus metals such as gold, platinum (Pt) or carbon are used to make them. Cyclic voltammetry (CV) analysis is used as a general method for obtaining basic and general information of electrochemical systems. This method, as a first step and an overview, can provide qualitative mechanism information that will guide the selection of a more advanced and accurate electrochemical method for studying the system. This technique was used in all stages of electrochemical tests in this study. Square wave voltammetry (SQW) analysis is a large-amplitude differential voltammetry technique and can provide quantitative mechanism information. Large and constant amplitude pulses are mounted on the increasing scanning potential. A schematic illustration of the three-electrode system is shown in Fig. 1(a). In this study, the SQW and EIS methods were used in $[Fe(CN)_6]^{-3/-4}$ media to measure the range of different concentrations of PSA. The biosensor is a measuring instrument that includes a biomaterial and an electric current conductor to generate a measurable signal depending on the analyte concentration, and can combine a molecular diagnostic mechanism with a physicochemical converter [12]. Aptamers have been used in the design of biosensors due to their high stability and selectivity [13]. The reason for using aptamer as a biological receptor is that unlike antibodies, the production of aptamers is in vitro and through chemical processes. Other advantages of aptamers over antibodies include non-cell-dependent chemical synthesis, low immunogenicity, low cost and higher half-life, and higher temperature resistance [13,14]. The ultimate goal of biosensors is to detect the specific signals of each disease, and nanoparticles have recently been widely used in the manufacture of biosensors, and these nanoparticles can react with the analyte in solution. Due to their small size, they easily penetrate into the cells and increase the detection range. Nanostructured materials act as guiding elements in biosensors, by providing more electroactive surface. Using functional groups increases the load stability of aptamers on the surface [15]. Graphene is widely used in the design and construction of biosensors due to its good physicochemical properties as well as high specific surface area and good biocompatibility and good thermal conductivity. Graphene-based biosensors have exhibited significant performance with excellent sensitivity, selectivity, stability and wide detection

range [16]. Graphene and its derivatives are nanoparticles with unique properties and have many applications in the design of nanobiosensors for cancer detection. Graphene is an allotrope of carbon, and carbon materials have already been used to manufacture electrochemical nanobiosensors. Graphene is a two-dimensional (2D) sheet of atoms of carbon in a hexagonal (honeycomb) configuration, the atoms of carbon in Graphene are linked by a sp2 or sigma (σ) hybrid, and Graphene is the newest member of the multidimensional graphite carbon family. Graphene sheets are formed by placing carbon atoms side by side, and in a Graphene sheet, each carbon atom is bonded to three other carbon atoms. One of the common methods in the synthesis of graphene is the production of GO and then its reduction and production of reduced graphene oxide. In this study, due to the greater stability of GO in water, and on the other hand, it has more functional groups than graphene and also more electron transfer in GO than graphene, was used GO. GO is one typical 2D structured and oxygenated planer molecular material. Recently, Graphene-based materials in the fabrication of nanobiosensors have been developed. rGO is a reduced form of GO that containins a π-conjugated system. g-C_3N_4 has a graphene-like layer structure, has good thermal and chemical stability and is cheap and easy to produce [17]. Furthermore, the optical properties and conductivity of g-C_3N_4, cause a great potential to be applied in optical and electrochemical biosensing. Au NPs have very significant properties, such as relative chemical stability, simple synthesis, high biocompatibility, and this nanoparticle also absorbs aptamer better. Au NPs can increase the sensitivity of the designed sensor. In fact, these nanoparticles act as a catalyst in the transfer of electrons between the analyte and the electrode surface. Due to the high conductivity of Au NPs and the fact that gold absorbs aptamer better, we have used these nanoparticles in biosensor design. In fact, by adding Au, the conductivity, absorption and biocompatibility properties are dramatically enhanced, which gives it a unique electrochemical performance [18]. An aptamer-based electrochemical for the detection of PSA using nanoparticles was presented in this work. For this purpose, first we synthesized nanoparticles and then using electrochemical characterization analysis in different modes of CV, SQW and EIS in $[Fe(CN)_6]^{-3/-4}$ media was examined to diagnosis PSA. Fig. 1(b) and Fig. 1(c) show the arrangement of electrodes in real measurements.

2- MATERIALS AND METHODS

Graphite powder used for the synthesis of GO, and $k_4Fe(CN)_6$, KMno4, H_2SO_4, $NaBH_4$, $HAucl_4.6H_2O$, H_2O_2, $C_6H_{12}O_6$, Urea used in this study. The aptamer for detecting prostate specific antigen with the TTTTTAATTAAAGCTCGCC ATCAAATA GCTTT OD2 HPLC 5' SH C6 sequence, in addition to bovine serum albumin (BSA) and fetal bovine albumin (FBS). The PSA used as a biomarker .Potentiostat /Galvanostat, manufactured by Ivium Technogies, was used for electrochemical tests. Electrodes include glass carbon electrode as a working electrode, platinum electrode as a counter electrode and Ag/AgCl electrode as a reference electrode. The device was used for electrochemical measurements by CV, SQW and EIS. Additionally, analyzes related to this study, such as Fourier-transform infrared spectroscopy (FT-IR), X-ray diffraction (XRD) test were performed in Laboratory and TEM was performed in Rastak Laboratory (Iran, https://www.partowrayan.com/).

2-1- Synthesis of Nanocomposite

GO was synthesized by the hummer method. In this method, 1g of graphite powder was added to 20 ml of H_2SO_4 and the solution was put in the ice bath. Later, 3g of $KMno_4$ was added to the above solution to make the solution color green. After a while, 50 ml of distilled water was added dropwise to the resulting solution, and after 10 min, 100 ml of distilled water was added. Finally, 35 ml of H_2O_2 was added to the solution and stirred for 24 h to well synthesize GO [19]. To synthesize the g-C_3N_4 nanoparticles, 5 g of Urea were poured into the plate, and were put in the oven at 450 to 550 °C for 4 h [20]. 0.3 g of Go was added to 100 ml of distilled water, and put the solution in the sonication bath for 10 min to make it homogenous. then 150 mg of the synthesized powder of g-C_3N_4 were added to the GO solution. Then, ultrasonic was performed for 10 min to obtain a solution of GO/g-N_4C_3 nanocomposite. 2.4 ml $HAucl_4.3H_2O$ (0.5 M) was added to the GO/g-C_3N_4 solution dropwise. In addition, after 30 min, 20 mg of $NaBH_4$ was added to the above solution, to form Au NPs on the surface of GO /g-C_3N_4. To prepare 100 µl of rGO/g-C_3N_4 /Au NPs-apt solution, 98 µl of rGO/g-C_3N_4 /Au (4.5 $mg.ml^{-1}$) solution was dissolved into 2 µl of aptamer solution, afterward for incubation it was put on the stirrer for 2 h and kept in the refrigerator for 24 h.

2-2- Characterization and Electrochemical Measurements

The working electrode surface was polished with alumina powder (Al_2O_3), subsequently was ensured that the electrode surface was clean by CV test in the potential range of -0.5 to 0.7 volts (v) with scan rate of 50 $mv.s^{-1}$, SQW in the potential range of -0.4 to 1 v with 100 mv amplifier and EIS test with 32 points. Frequency in the range of 0.01 to 100000 Hz in $[Fe(CN)_6]^{-3/-4}$ media (0.2 M) . was dropped 4 µl of rGO/g-C_3N_4 and rGO /g-C_3N_4 /Au NPs solution on the surface of the other electrodes and recorded the analysis. To ensure the aptamer binding to rGO/g-C_3N_4 /Au NPs, 4 µl of rGO/g-C_3N_4/Au NPs-apt solution was dropped on the working electrode surface and the analysis CV, SQW and EIS was recorded. Additionally, 10 µl PSA (7.5 $pg.ml^{-1}$) was dropped on the electrode surface containing rGO/g-C_3N_4/Au NPs-apt to ensure analyte the binding to aptamer. After 30 min, the non-aptamer-bound analyte were washed with PBS (pH=7.4) and the above tests were repeated.

2-3-Concentration Analysis in $[Fe(CN)_6]^{-3/-4}$ Media

For measurement of various PSA concentrations in $[Fe(CN)_6]^{-3/-4}$ media, after assuring that the working electrode surface was clean, 4 µl of rGO/g-C_3N_4/Au NPs-apt solution was dropped on the working electrode surface. After drying

the electrode surface, was dropped 10 µl of PSA (2.5 pg.ml^{-1}) on the electrode surface and thereupon washed the unbound analyte with PBS (pH=7.4) and were performed CV, SQW and EIS analysis in $[Fe(CN)_6]^{-3/-4}$ media. Eventually, were performed all tests for different concentrations of PSA (5, 7.5, 10, 12.5 pg.ml^{-1}) from low to high concentrations without clearing the electrode surface.

2-4- Selectivity Analysis in $[Fe(CN)_6]^{-3/-4}$ Media

Selectivity analysis was performed in the $[Fe(CN)_6]^{-3/-4}$ media, dropped 4 µl of rGO/g-C_3N_4/Au NPs-apt on the working electrode surface, and performed the SQW test (-0.4 to 1 v with 100 mv amplifier). Subsequently, 10 µl of rGO/g-C_3N_4/Au NPs-apt was dropped on the working electrode surface. After 30 min, the electrode surface was washed with PBS (PH=7.4), and the SQW test was recorded for various materials such as $C_6H_{12}O_6$ (90 mg.ml^{-1}), BSA (7 µg.ml^{-1}), FBS (5 ng.ml^{-1}), CA15-3, PSA (7.5 pg.ml^{-1}).

2-5- Time Profile Analysis in $[Fe(CN)_6]^{-3/-4}$ Media

After cleaning the electrode surface, the rGO/g-C3N4/Au NPs-apt solution was incubated for 15 min and 4 µl of the above solution was dropped on the electrode surface. After drying the electrode surface, 10 µl of the PSA (7.5 pg. ml^{-1}) was dropped on the electrode surface. After multiple times, (10, 20, 30, 40, 50, 60 min), the test was repeated for separate electrodes and finally the excess analyte was washed with PBS solution, and the SQW test was recorded.

3- RESULTS AND DISCUSSION

Fig. 2(a), Fig. 2(b), Fig. 2(c), Fig. 2(d), and Fig. 2(e) show the morphology and structure of the synthesized materials. The X-ray pattern of GO shows that a sharp peak appears at 2θ=25.21º. Since the distance between GO layers is directly related to its oxidation and with increasing oxidation rate, the distance between GO layers' increases. Furthermore, according to the peak observed in Kaur et al. research, the synthesis of GO correctly was found [25]. In XRD of g-C_3N_4, peaks at 2θ=27.68 º and 2θ=11.46º are shown, which are related to the reflection of (002) and (100). Reflects of (002) is related to the interplate accumulation of aromatic systems, and (100) shows the repetition of successive triazine networks. The peak observed at 2θ=27.2º, which corresponds to the substance GO/g-C_3N_4, indicates that the g-C_3N_4 particles are correctly located on GO. Moreover, Peaks at 2θ=44.96º, 2θ=39.13º, 2θ=33.81º, 2θ=27.67º are shown, which correspond to the material GO/g-C_3N_4/Au. The sharpening of the peaks in the GO/g-C_3N_4/Au nanocomposite indicates that the Au NPs are well placed on the GO/g-C_3N_4 sheets Fig. 2(a).

Transmission electron microscopy (TEM) are special tools in detecting the structure and morphology of materials that make microstructural studies of materials with high resolution and magnification possible. Since most nanoparticles agglomerate after synthesis, these materials must be dispersing before being observed in the TEM test. To prepare these samples, first an amount of the synthesized powder is placed in a jar containing a suitable dispersant (ethanol, acetone, distilled water, etc.) of the sample. It should be noted that a suitable dispersant is a dispersant that does not react with the sample. The glass containing the nanoparticles is then placed in an ultrasonic device and a suitable time and power is applied to disperse the nanoparticles; This timelapse can be between 1 and 30 min, depending on the sample. Afterwards, with a micropipette, take a few drops from the sample glass and pour it on the appropriate grade, which is the nanoparticle holder for the TEM device, and allow the dispersant to evaporate from the grade for a few minutes. Later the grade is taken into the TEM device. Well scanning electron microscopy(SEM) images show the porosity of GO plates. In this study, the morphology and surface properties of synthesized GO were investigated using scanning and transmission electron microscopy images. The SEM and TEM images of the synthesized GO are shown in Fig. 2(b) and Fig. 2(d). GO layers are well visible in these shapes, which is evidence of the conversion of graphite plates to graphene oxide layers. Additionally, synthesized graphene oxide is clearly recognizable in the form of monolayer, which indicates the quality of synthesized GO and The presence of wrinkles is a feature of monolayer GO. GO cannot be seen clearly from the TEM image of GO/g-C3N4 in Fig1 2(c).

FTIR analysis was used to study the structure of synthesized materials and to identify functional groups. Fig. 2(e), shows the GO FTIR, the specific peaks in the range of 1050 cm^{-1} represent the C-O group, and in the 3000cm^{-1} to 3700cm^{-1} range the hydroxyl group (C-OH). Additionally, the peak in 3435cm^{-1} is related to the vibrational state of O-H. Peaks in the range of 1200cm^{-1} to 1620cm^{-1}, which indicate the C=N bond and the tensile state of the C-N aromatic bonds, can be seen in the FT-IR of the g-C_3N_4 particle, and the peaks of 2012cm^{-1} and 3328cm^{-1} are NH and NH_2 tensile vibrations. The peak shown in region 808cm^{-1}, which relates to the GO/g-C_3N_4 nanocomposite, indicates triazine units, and due to the formation of g-C_3N_4 layers on the surface of GO, only g-C_3N_4 peaks are observed Fig. 2(e).

To characterize the synthesized materials, CV analysis was used in the range of -0.5 to 0.7 v with a scan rate of 50 mv.s^{-1}, SQW in the potential range of -0.4 to 1 volts and EIS test with 32 points Frequency in the range of 0.01 to 100000 Hz in $[Fe(CN)_6]^{-3/-4}$ media. According to CV Fig. 3(a) and SQW Fig. 3(b) tests, due to the lack of reducing materials when the electrode surface is bare the most current flows through the electrode surface. Later, by adding GO to the electrode surface, the current decreases slightly, and when we add g-C_3N_4, the current increases due to the increased conductivity of GO, and this conductivity increases with the addition of Au NPs. Finally, by adding a specific aptamer, the current is reduced. Later by adding PSA, the current is reduced, and it can be concluded that the designed nanobiosensor has worked properly for Fig. 3(a), Fig. 3(b). In the EIS analysis, by adding GO, the resistance of the electrode surface has increased to the state where the surface is bare, then by adding g-C_3N_4 nanoparticles and Au to the electrode surface, the resistance is reduced. Finally by adding aptamer

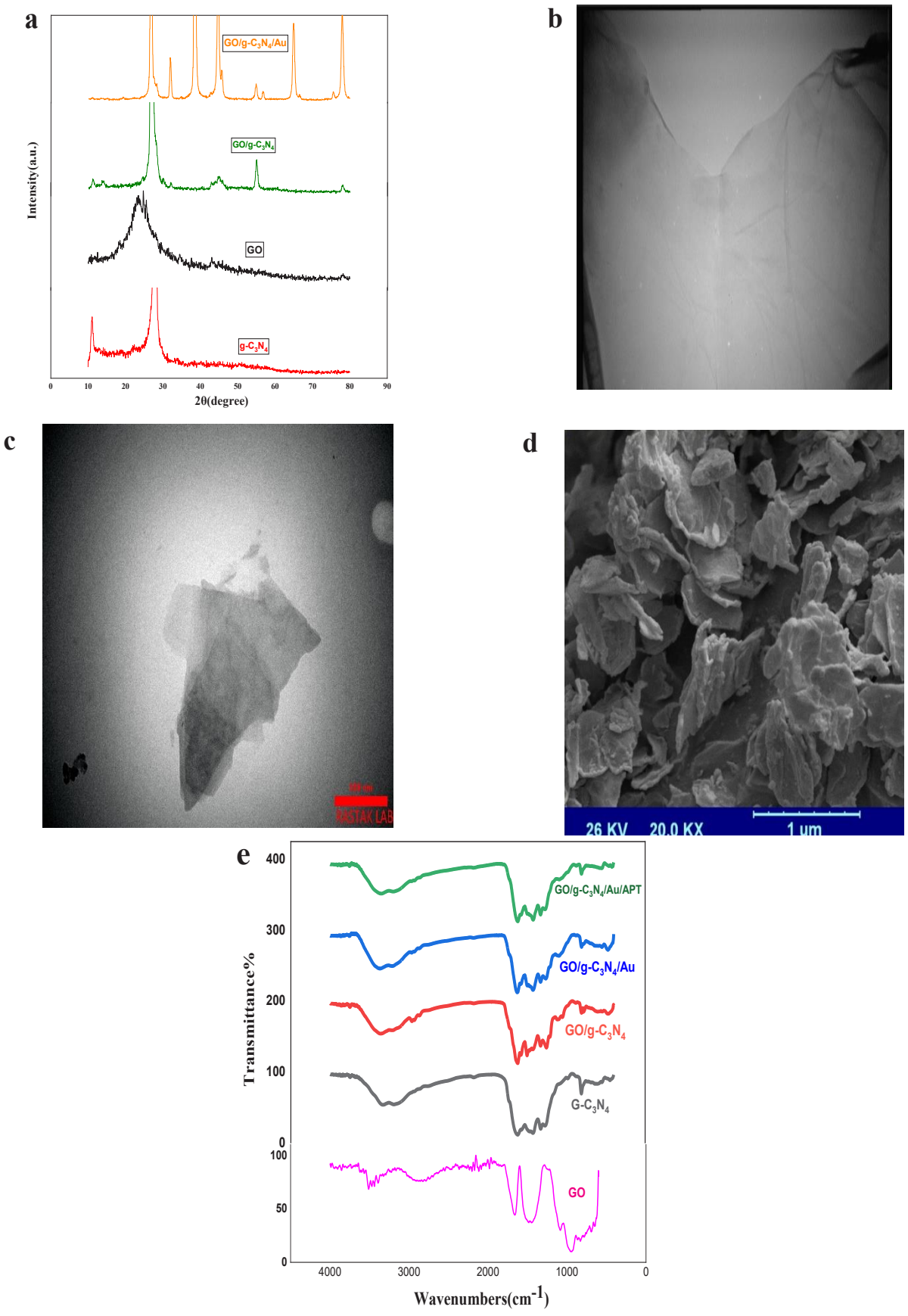

Fig. 2. (a) XRD pattern of GO, g-C_3N_4, GO /g-C_3N_4, GO /g-C_3N_4 / Au. (b) TEM of GO. (c) TEM of GO/g-C_3N_4. (d) SEM of GO. (e) FTIR of GO, g-C_3N_4, GO/g-C_3N_4, GO/g-C3N4 /Au, GO /g-C_3N_4 /Au /apt.

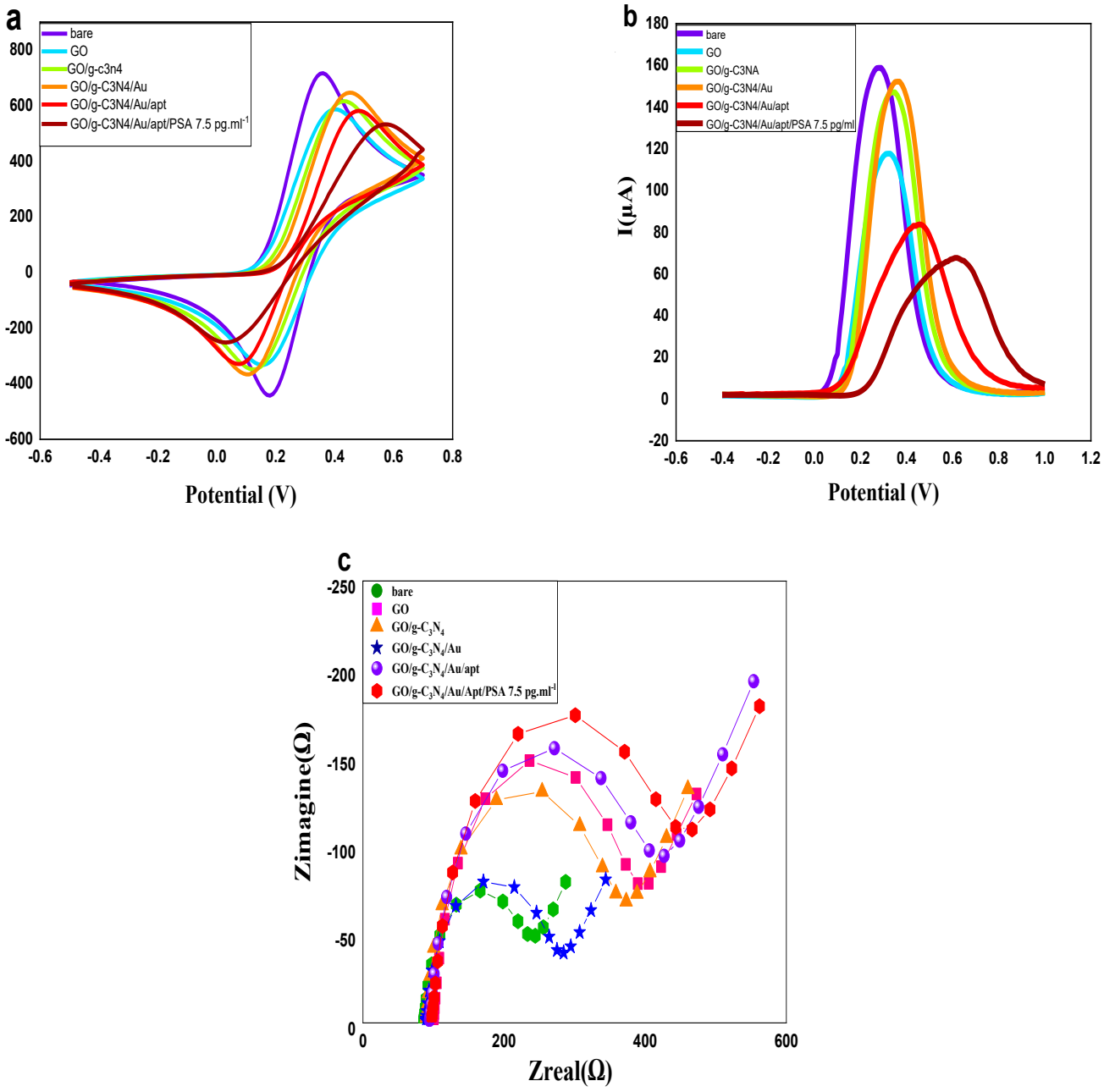

Fig. 3. The electrochemical characterization of the nanocomposite, (a) CV analysis in $[Fe(CN)_6]^{-3/-4}$ media. (b) SQW analysis in $[Fe(CN)_6]^{-3/-4}$ media. (c) EIS analysis in $[Fe(CN)_6]^{-3/-4}$ media.

and PSA, the resistance is increased in Fig. 3(c).

To ensure analyte binding (PSA) to aptamer, CV, SQW and EIS analysis were recorded with the same parameters at different PSA concentrations. As it is known in CV Fig. 4(a) and SQW Fig. 4(b), analysis has decreased the electrochemical peak with increasing PSA concentration and the trend of decreasing current is due to the enhancement of resistance. Considering the calibration curve for SQW analysis, we conclude that the linear response with high correlation coefficient $R^2 = 0.99269$ is acceptable in Fig. 4(c). According to the EIS analysis curve of Fig. 4(d) for different concentrations of PSA, it is clear that with increasing the PSA concentrations, the resistance of the electrode surface and the diameter of the semicircle have increased. The limit of detection is the lowest concentration that a method can detect with a certain degree of certainty and LOD is the level of concentration where detecting PSA is difficult. The LOD of this biosensor follows Eq. (1):$LOD = \frac{\eth}{b}$)

Where ***b*** is the slope of the calibration curve in the SQW technique and $\eth$ is the blank standard deviation. using Equation (1), LOD was obtained 1.67 $pg.ml^{-1}$.

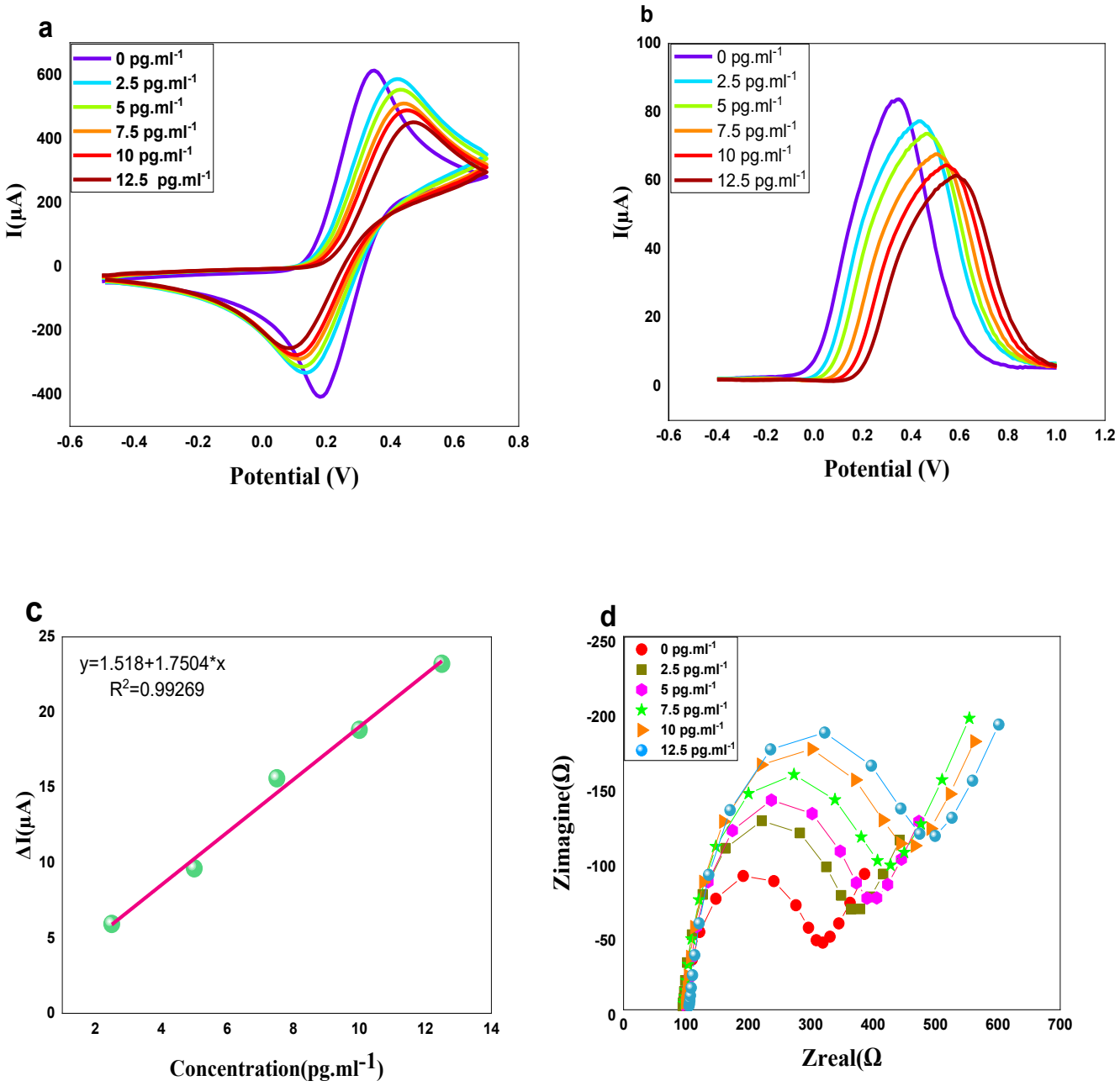

Fig. 4. (a) The CV analysis, (b) and SQW analysis for various concentrations of PSA in $[Fe(CN)_6]^{-3/-4}$ media. (c) calibration curve derived from SQW. (d) EIS in $[Fe(CN)_6]^{-3/-4}$ media at various concentration of PSA.

The selectivity and specificity of a biosensor play a very important role in the detection of biological samples. Fig. 5(a) shows the selectivity of various materials (FBS, BSA, PSA, CA15-3, $C_6H_{12}O_6$). According to these graphs, it is clear that the response of the designed biosensor to FBS, BSA, CA15-3, $C_6H_{12}O_6$ in $[Fe(CN)_6]^{-3/-4}$ media is very low, while the response of the biosensor to PSA is high, which is due to the high selectivity of the sensor. According to Fig. 5(b), we had the best protein binding (PSA) to aptamer at 30 min, and this time is adequate for incubation of PSA and after 30 min, the unobserved effect in the PSA absorption.

Table 1 summarizes the various studies of the design of biosensors for the diagnosis of PSA. According to Table 1, L. Hen et al. fabricated an Electrochemical biosensor for low level detection of PSA based on rGO/Ag NPs. Moreover, the modified electrode in the present study shows good performance for highly sensitive and selective detection of PSA compared to L. Hen's study [22]. In other research, S. Rafique et al. used Au-NS for electrochemical determination of PSA. Accordingly, the biosensor is fabricated for selective detection of PSA with high sensitivity and 0.023 ng. mL^{-1} limit of detection [29]. E. Heydari-Bafrooei et al. have successfully

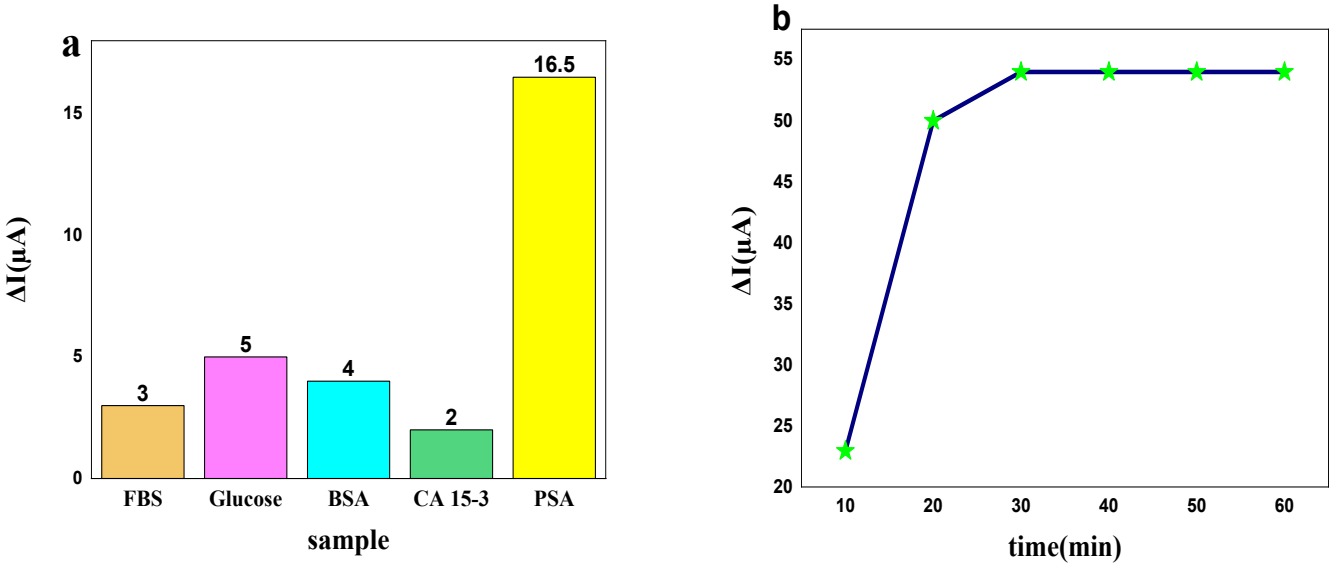

Fig. 5. (a) The selectivity of designed nanobiosensor in $[Fe(CN)_6]^{-3/-4}$ media. (b) time profile of designed biosensor.

Table 1. comparison of reported electrochemical biosensor for detection of PSA.

Electrode material	Linear range (as reported)	Detection limit (as reported)	References
CNT/ Au NPs	(0.01 – 0.5 ng.ml^{-1})	7 pg.ml^{-1}	[21]
rGO –Ag NPs	(1-1000 ng.ml^{-1})	10 pg.ml^{-1}	[22]
rGO/Fe3O4/Cu2O NSs and Ag@ RF-Ag NPs	(0.01 – 100 ng.ml^{-1})	6.2 pg.ml^{-1}	[23]
MoS_2QDs@g-C_3N_4@CS-AuNPs	-	0.71 pg.ml^{-1}	[26]
GR – Au NPs	(0 – 10 ng.mL^{-1})	590 pg.mL^{-1}	[27]
PtCu @ rGO/g-C_3N_4	(50 fg.mL^{-1} – 40 ng.mL^{-1})	16.6 fg.mL^{-1}	[28]
Au –NS electrode	(0.5 – 100 ng.mL^{-1})	0.023 ng.mL^{-1}	[29]
MWCNT-AuNPs/CS-AuNPs/rGO-AuNPs	(0.01-100.00 ng. mL^{-1})	6.0 pg. mL^{-1}	[30]
rGO/ g-C_3N_4/ Au	(2.5 - 12.5 pg.ml^{-1})	1.67 pg.ml^{-1}	This study

designed an Electrochemical Aptamer-Based biosensor for PSA determination. In this study MWCNT-AuNPs/CS-AuNPs/rGO-AuNPs were used to increase the electrical conductivity and surface area. Based on the calibration curve, the detection limit of 6.0 pg.ml^{-1} and the linear range of 0.01-100.00 ng. mL^{-1} was obtained. Additionally, according to the present work, it seems that the biosensor with low limit of detection (1.67 pg.ml^{-1}) and wide linear range may be a suitable device to diagnose prostate cancer [30].

4- CONCLUSION

In this work, an aptamer-based electrochemical biosensor was presented for rapid diagnosis of PSA. Electrochemical biosensor designed with good stability and high selectivity, detects the desired PSA compared to other materials. Attempts have also been made to use nanoparticles to establish a specific PSA-specific aptamer. And Electrochemical analysis was performed in $[Fe(CN)_6]^{-3/-4}$ media and the LOD is 1.67 pg.ml^{-1}. decoration of Au NPs on the rGO/g-C_3N_4 caused a suitable substrate for easier placement of aptamer on its surface, as well as increasing the conductivity of nanocomposite, which significantly helps to improve the performance and sensitivity of the biosensor. The results showed that the use of rGO/g-C_3N_4/Au NPs significantly enhanced the LOD and linearity range.

REFERENCES

[1] S. McGuire, "World Cancer Report 2014. Geneva, Switzerland: World Health Organization, International Agency for Research on Cancer, WHO Press, 2015," *Adv. Nutr.*, vol. 7, no. 2, pp. 418–419, 2016.

[2] A. Rahi, N. Sattarahmady and H. Heli (2016). Label free electrochemical aptasensing of the human prostate-specific antigen using gold nanospears, Talanta. 156, pp. 218–224.

[3] S. M. Cruz, A. F. Girão, G. Gonçalves and P.A. Marques (2016). Graphene: The Missing Piece for Cancer Diagnosis? Sensors. 16, pp. 137.

[4] Ruddon R.W.)2007(. Cancer Biology. Oxford University Press, USA .

[5] W. J. Catalona, "Prostate Cancer Detection in Men With Serum PSA Concentrations of 2.6 to 4.0 ng/mL and Benign Prostate Examination," *Jama*, vol. 277, no. 18, p. 1452, 1997

[6] [6]H. Lilja, J. Oldbring, G. Rannevik, and C. B. Laurell, "Seminal vesicle-secreted proteins and their reactions during gelation and liquefaction of human semen.," *J. Clin. Invest.*, vol. 80, no. 2, pp. 281–285, 1987

[7] S. M. Totten *et al.*, "Multi-lectin Affinity Chromatography and Quantitative Proteomic Analysis Reveal Differential Glycoform Levels between Prostate Cancer and Benign Prostatic Hyperplasia Sera," *Sci. Rep.*, vol. 8, no. 1, pp. 1–13, 2018.

[8] I. E. Tothill, "Biosensors for cancer markers diagnosis," *Semin. Cell Dev. Biol.*, vol. 20, no. 1, pp. 55–62, 2009.

[9] M. Ferrari, R. Bashir, and S. Wereley, *BioMEMS and biomedical nanotechnology; Volume IV: Biomedical sensing, processing and analysis*. 2007.

[10] R. E. Madrid, R. Chehín, T.-H. Chen, and A. Guiseppi-Elie, "Biosensors and Nanobiosensors," no. March, pp. 391–462, 2017.

[11] M. Pumera, "Nanocarbon electrochemistry," *SPR Electrochem.*, vol. 11, pp. 104–123, 2013.

[12] O. Lazcka, F. J. Del Campo, and F. X. Muñoz, "Pathogen detection: A perspective of traditional methods and biosensors," *Biosens. Bioelectron.*, vol. 22, no. 7, pp. 1205–1217, 2007.

[13] S. M. Khoshfetrat and M. A. Mehrgardi, "Amplified detection of leukemia cancer cells using an aptamer-conjugated gold-coated magnetic nanoparticles on a nitrogen-doped graphene modified electrode," *Bioelectrochemistry*, vol. 114, pp. 24–32, 2017.

[14]] Rna Aptamers 193 [14]," vol. 318, no. 1997, pp. 193–214, 2000.

[15] P. R. Nair and M. A. Alam, "Screening-limited response of NanoBiosensors," *Nano Lett.*, vol. 8, no. 5, pp. 1281–1285, 2008.

[16] Feng L, Chen Y, Ren J, Qu X (2011) A graphene functionalized electrochemical aptasensor for selective label-free detection of cancer cells. Biomaterials 32:2930–2937.

[17] S. Cao and J. Yu, "g-C_3N_4-Based Photocatalysts for Hydrogen Generation," *J. Phys. Chem. Lett.*, vol. 5, pp. 2101–2107, 2014.

[18] M. Omidi, G. Amoabediny, F. Yazdian, and M. Habibi-Rezaei, "Protein-based nanobiosensor for direct detection of hydrogen sulfide," *Epl*, vol. 109, no. 1, 2015.

[19] Chen J, Yao B, Li C, Shi G (2013) An improved hummers method for eco-friendly synthesis of graphene oxide. Carbon 64:225–229.

[20] D. Ma, J. Wu, M.C. Gao, Y.J. Xin, T.J. Ma, Y.Y. Sun, Fabrication of Z-scheme g-C3N4/RGO/Bi2WO6 photocatalyst with enhanced visible-light photocatalytic activity, Chem. Eng. J. 290 (2016) 136–146.

[21] J. Tian, J. Huang, Y. Zhao, and S. Zhao, "Electrochemical immunosensor for prostatespecific antigen using a glassy carbon electrode modified with a nanocomposite containing gold nanoparticles supported with starch-functionalized multi-walled carbon nanotubes," Microchim. Acta, vol. 178, no. 1–2, pp. 81–88, 2012.

[22] L. Han et al., "Enhanced conductivity of rGO/Ag NPs composites for electrochemical immunoassay of prostate-specific antigen," Biosens. Bioelectron., vol. 87, pp. 466–472, 2017.

[23] Y. Zhao, H. Liu, L. Shi, W. Zheng, and X. Jing, "Electroactive Cu2O nanoparticles and Ag nanoparticles driven ratiometric electrochemical aptasensor for prostate specific antigen detection," Sensors Actuators, B Chem., vol. 315, no. January, p. 128155, 2020.

[24]]P. S. Nnamchi and C. S. Obayi, *Electrochemical characterization of nanomaterials*. Elsevier Ltd., 2018.

[25] Navneet Kumar, Vimal Chandra Srivastava. Simple Synthesis of Large Graphene Oxide Sheets via Electrochemical Method Coupled with Oxidation Process. *ACS Omega* **3**:8, 10233-10242, 2018.

[26] F. Duan, S. Zhang, L. Yang, Z. Zhang, L. He, and M. Wang, "Bifunctional aptasensor based on novel two-dimensional nanocomposite of MoS2 quantum dots and g-C3N4 nanosheets decorated with chitosan-stabilized Au nanoparticles for selectively detecting prostate specific antigen," *Anal. Chim. Acta*, vol. 1036, pp. 121–132, 2018.

[27] H.D. Jang, S.K. Kim, H. Chang, J.W. Choi, 3D label-free prostate specific antigen (PSA) immunosensor based on graphene-gold composites, Biosens. Bioelectron. 63 (2015) 546–551. https://doi.org/10.1016/j.bios.2014.08.008. 2015.

[28] J. Feng, Y. Li, M. Li, F. Li, J. Han, Y. Dong, Z. Chen, P. Wang, H. Liu, Q. Wei, A novel sandwich-type electrochemical immunosensor for PSA detection based on PtCu bimetallic hybrid (2D/2D) rGO/g-C3N4, Biosens. Bioelectron. 91 (2017) 441–448. https://doi.org/10.1016/j.bios.2016.12.070, 2016.

[29] S. Rafique, W. Bin, A.S. Bhatti, Electrochemical immunosensor for prostate-specific antigens using a label-free second antibody based on silica nanoparticles and polymer brush, Bioelectrochemistry. 101 (2015) 75–83. https://doi.org/10.1016/j.bioelechem.2014.08.001, 2014.

[30]]Heydari-Bafrooei E, Askari S. Detection of Prostate Specific Antigen Using an Electrochemical Aptamer-Based Biosensor. *Univ Med Sci* 2018; 17 (2): 115-30.2018. [Farsi]

HOW TO CITE THIS ARTICLE

F.Saeidi Tabar, M.Pourmadadi, F.Yazdian, H.Rashedi, Design of a Novel Electrochemical Nanobiosensor for the Detection of Prostate Cancer by Measurement of PSA Using Graphene-based Materials , AUT J. Elec. Eng., 53(2) (2021) 213-222.

DOI: 10.22060/eej.2021.19463.5396